

Original Research

Heme Oxygenase-1 Alleviates Ischemia-Reperfusion Injury by Inhibiting Hepatocyte Pyroptosis after Liver Transplantation in Rats

Tao Wang^{1,†}, Yuan Fang^{1,†}, Xiaoli Zhang², Yang Yang³, Li Jin¹, Zhitao Li¹, Yinglei Miao^{4,5}, Zhong Zeng^{1,*}, Hanfei Huang^{1,*}¹Organ Transplantation Center, the First Affiliated Hospital of Kunming Medical University, 650032 Kunming, Yunnan, China²Gastrointestinal and hernia surgery, the First Affiliated Hospital of Kunming Medical University, 650032 Kunming, Yunnan, China³Otorhinolaryngology Head and Neck Surgery, Baoshan People's Hospital, 678000 Baoshan, Yunnan, China⁴Department of Gastroenterology, The First Affiliated Hospital of Kunming Medical University, 650032 Kunming, Yunnan, China⁵Yunnan Province Clinical Research Center for Digestive Diseases, 650032 Kunming, Yunnan, China*Correspondence: zengzhong@kmmu.edu.cn (Zhong Zeng); huanghanfei@kmmu.edu.cn (Hanfei Huang)

†These authors contributed equally.

Academic Editor: Moo-Ho Won

Submitted: 28 February 2023 Revised: 6 May 2023 Accepted: 23 May 2023 Published: 31 October 2023

Abstract

Objective: Heme oxygenase-1 (HO-1) is a protein involved in the inflammatory response following ischemia-reperfusion injury (IRI). Evidence suggests that pyroptosis plays an important role in IRI. However, the underlying mechanism between HO-1 and pyroptosis in IRI requires further investigation. **Methods:** Using the “two-cuff” method, a Sprague Dawley rat model of liver transplantation (LT) was established using livers from donors after circulatory death. An automatic biochemical analyzer was used to detect serum alanine transaminase (ALT) and aspartate aminotransferase (AST) levels and evaluate liver function. Paraffin sections of the rat liver were stained with hematoxylin-eosin (HE) to observe the degree of pathological damage. An enzyme-linked immunosorbent assay was used to detect serum levels of interleukin (IL)-1 β and IL-18. Moreover, western blotting was used to analyze the expression of HO-1, pro-caspase-1, p22, full-gasdermin D (GSDMD), and cleaved-N-GSDMD in the liver. Immunohistochemistry was used to detect NLRP3 expression. **Results:** HO-1 expression was time-dependent with IRI. HE staining and Suzuki score showed that necrosis was more severe at 6 h after IRI than in controls. Reactive oxygen species (ROS), ALT, and AST levels in the reperfusion were significantly higher at 6 h after IRI. Similar to HO-1 expression, pro-caspase-1, p22, and GSDMD expression in the reperfusion was time-dependent and was significantly higher at 6 h. Compared with the HO-1-shRNA (short hairpin RNA) group, the HO-1 overexpression group significantly inhibited ROS, p22, GSDMD, IL-1 β , IL-18, ALT, and AST. Immunohistochemistry revealed that NLRP3 levels were the highest in the HO-1 overexpression group. **Conclusions:** HO-1 improved the survival rate and IRI recovery after LT in rats. This study demonstrates that HO-1 inhibits hepatocyte pyroptosis, thereby reducing IRI after LT.

Keywords: heme oxygenase-1; cardiac death donor; liver transplantation; ischemia-reperfusion injury; pyroptosis

1. Background

Liver diseases are often associated with multi-factorial liver insufficiency and irreversible damage to organs, owing to which such diseases are often associated with a high risk of mortality. Often, liver transplantation (LT) is the only curative treatment for these diseases [1]. Donors after circulatory death (DCD) have recently been the main source of organs. However, DCD livers are frequently exposed to a long ischemic period [2]. This often results in hepatic ischemia-reperfusion injury (IRI), which is the main risk factor for early allograft dysfunction and acute or chronic rejection. Additionally, IRI is an important factor in the shortage of donor organs [3]. Since the mechanism underlying liver IRI is not well understood, it is necessary to study the mechanism of graft IRI to improve the clinical outcomes of LT. A variety of damage-associated molecular patterns (DAMPs) upregulate Kupffer cells (KCs) to form several inflammatory complexes through different pattern recogni-

tion receptors (PRRs) [4]. NLRP3 is one such PRR that induces the autohydrolysis of two adjacent pro-caspase-1 molecules to produce caspase-1, an enzyme that cleaves the precursors of interleukin (IL)-1 β and IL-18 [5]. Hepatic IRI is characterized by cell death that is mediated by processes such as apoptosis, necrosis, iron death, and pyroptosis [6]. Specifically, pyroptosis is closely associated with the mechanisms underlying hepatic IRI. Pyroptosis relies on the activation of inflammasome-mediated caspase-1, and the insertion of gasdermin D (GSDMD) leads to the formation of pores in the plasma membrane. In turn, intracellular proteins are released from the cells, resulting in ion decompensation. Furthermore, water influx from the surroundings into the cell leads to cell swelling [7]. Activated caspase-1 can additionally cleave GSDMD to produce GSDMD-N and -C [8,9]. In addition, following oxidative stress response, mitochondria produce excessive oxygen free radicals, among which reactive oxygen species (ROS) levels are



significantly increased [10]. The overexpression of ROS can promote the maturation of NLRP3 and ultimately mediate the occurrence of pyroptosis through caspase-1 [11].

Heme oxygenase-1 (HO-1) is the stress-inducing, rate-limiting enzyme that catalyzes the oxidation degradation of heme into carbon monoxide, iron, and biliverdin [12]. Moreover, HO-1 has been demonstrated to have antioxidant and cytoprotective activity in various models of organ damage and diseases of the lung, kidneys, heart, and liver [13]. In addition, previous studies have shown that HO-1 plays a vital role in the pathogenesis of IRI by enhancing the ability of liver cells to resist oxidative stress and by stabilizing mitochondrial function. In patients undergoing orthotopic LT, pretreatment with adenovirus, which interferes with HO-1 expression, significantly improves IRI in Sprague Dawley (SD) rats and promotes the recovery of liver function [10,14,15].

Based on this evidence, the present study aims to determine whether HO-1 could alleviate hepatic IRI in DCD rats and improve liver function by inhibiting hepatocyte pyroptosis.

2. Materials and Methods

2.1 Ethics Statement

This study purchased 208 male SD rats (150–180 g; 5–6 weeks old; SPF grade) from Beijing HuaFuKang Bioscience Company (Beijing, China). The animal protocol was approved by the Institutional Animal Care and Use Committee of Kunming Medical University (Kunming, China; KMMU2020189). All animal experiments were performed in compliance with the National Institute of Health guidelines for animal experimentation.

2.2 SD Rat Surgery Procedure

The SD rat LT model was established using the “two-cuff” technique reported by Kamada *et al.* [16], which has been detailed in the **Supplementary Materials**. The study has been reported per the ARRIVE guidelines [17].

2.3 Adeno Associated Virus Transfection Efficiency Test

To explore the transfection efficiency of adeno-associated virus (AAV), 25 SD rats were randomly allocated into five groups: shRNA-NC, shRNA-HO-1, AAV-NC, AAV-HO-1, or normal groups. Rats in all groups were injected with 200 μ L of AAV titer (2.5×10^9 mg/ μ L; Hanbio Biotechnology, Shanghai, China) via the tail vein. The AAV-HO-1, shRNA-HO-1, and the respective blank control virus vectors were transduced into SD rats for 21 days.

2.4 Study Design

Of the 208 rats, 88 were injected with AAV via the tail vein and were randomly divided into the following six groups: sham (n = 8, only laparotomy); DCD (n = 16, donors were injected with normal saline); DCD + shRNA-NC (n = 16, donors underwent transduction with HO-1-

shRNA empty-loaded virus); DCD + shRNA-HO-1 (n = 16, donors underwent transduction with HO-1-shRNA-AAV); DCD + AAV-NC (n = 16, donors underwent transduction with HO-1-overexpressing empty-loaded virus); or DCD + AAV-HO-1 (n = 16, donors underwent transduction with HO-1-overexpressing AAV).

In addition, to explore whether HO-1 induces pyroptosis in hepatic IRI and whether this effect is observed in a time-dependent manner, 54 rats were randomly allocated into five groups: normal group (n = 6) and hepatic ischemia-reperfusion (IR) groups with reperfusion for 6 h (DCD + IR6h), 24 h (DCD + IR24h), 72 h (DCD + IR72h), or 168 h (DCD + IR168h) (each, n = 12).

Furthermore, 66 SD rats were randomly divided into the following six groups for assessing HO-1-related cell pyroptosis at 6 h (n = 12, i.e., 6 pairs). The groups were as follows: sham (n = 6, only underwent laparotomy), DCD (n = 12, the donor was injected with normal saline via the tail vein), DCD + shRNA-NC (n = 12, donor underwent transduction with HO-1 shRNA AAV via the tail vein); DCD + shRNA-HO-1 (n = 12, donor underwent transduction with HO-1 shRNA AAV via the tail vein); DCD + AAV-NC (n = 12, donor underwent transduction with HO-1-overexpressing AAV empty virus via the tail vein); and DCD + AAV-HO-1 (n = 12, donor underwent transduction with HO-1-overexpressing AAV via the tail vein).

2.5 Biochemical Assay and Measurement of Cytokines

The serum alanine transaminase (ALT) and aspartate aminotransferase (AST) levels in SD rats were measured using a fully automatic biochemical analyzer (BIO-RAD, Hercules, CA, USA), expressed in U/L. In addition, serum IL-1 β and IL-18 levels in blood from the coronary artery (ERC007.96, ERC010.96, Neobioscience Technology Company, Shenzhen, China) were assessed using a commercially available enzyme-linked immunosorbent assay kit, according to the manufacturer’s instructions. Optical density was measured at 450 nm.

2.6 Flow Cytometry

Initially, 50 μ g of fresh SD rat liver tissue was weighed and then homogenized and filtered into a cell suspension. This suspension was centrifuged, and then the obtained pellet was mixed with an appropriate volume of DCFH-DA (S0033S, Beyotime Biotechnology, Shanghai, China), which was diluted with serum-free culture medium (1:1000) to make a final concentration of 10 μ mol/L. Subsequently, the medium was incubated at 37 $^{\circ}$ C for 20 min. The cells were then washed thrice with a serum-free cell culture medium to remove the DCFH-DA that had not entered the cells. The ROS-positive control group was treated with Rosup for 20–30 min. Then, flow cytometry (excitation wavelength: 488 nm, emission wavelength: 525 nm) was used to detect the fluorescence intensity before and after stimulation.

2.7 Histological and Immunohistochemical Study

For histological analyses, the liver tissues of rats were fixed with 4% paraformaldehyde for 48 h. The fixed liver samples were then dehydrated, embedded in paraffin, and cut into <3 mm thick sections ($n = 3$ for each liver). The sections were stained with hematoxylin-eosin (HE) for pathological evaluation.

In addition, fresh liver tissues were embedded in optimum cutting temperature compound, frozen, sectioned, and observed under an inverted fluorescence microscope.

For immunohistochemical analyses, liver tissues were embedded in paraffin and sliced, as mentioned above. The sections obtained were incubated at 65 °C for 20 min and were deparaffinized using a gradient of xylene and ethanol solution, followed by treatment with 0.01 mol/L (pH 6.0) citrate buffer for antigenic repair. Subsequently, the sections were treated with 3% hydrogen peroxide to quench endogenous peroxidase activity and, after 15 min, were blocked with 5% bovine serum albumin for 30 min. The sections were then incubated with NLRP3 antibody (dilution ratio: 1:200; 19771-1-AP, ProteinTech, Wuhan, Hubei, China) overnight at 4 °C. Following this, the sections were treated with secondary antibody for 50 min and incubated with DAB. The sections obtained were observed under an optical microscope (Olympus, cymml-3ptxcj-004, Hamburg, Germany). All images shown in the results represent at least three images of each liver. The Liver Suzuki scoring standard was used [18,19]. ImageJ software (Rasband WS, ImageJ, V 1.8.0, National Institutes of Health, Bethesda, MD, USA) was used to quantify the stained areas in sections.

2.8 Western Blot Analysis

As reported previously [20], the membrane was blocked with 5% skim milk for 2 h and then incubated with rabbit anti-HO-1 (dilution ratio 1:1000; E6Z5G, Cell Signaling Technology, Danvers, MA, USA), anti-caspase-1 (dilution ratio 1:1000; EPR19672, Abcam, Cambridge, UK), anti-GSDMD (dilution ratio 1:1000; EPR20859, Abcam), and NLRP3 (dilution ratio 1:1000; 19771-1-AP, Proteintech) overnight at 4 °C. After washing thrice with Tris-Buffered Saline and Tween 20 (TBST), the membrane was incubated with IgG antibody at room temperature for 2 h. The membrane was completely covered with the developing liquid and observed using the gel imaging system (Monad, GD50202, Suzhou, China).

2.9 Reverse Transcription-Quantitative Polymerase Chain Reaction (RT-qPCR)

RT-qPCR was performed as described previously using the SuperReal PreMix Plus (SYBR Green, Roche, Mannheim, Germany) kit and the Mx3005 P Real-Time PCR System (Agilent, Santa Clara, CA, USA) [21]. Briefly, total RNA from liver tissues was extracted using TRIzol (Invitrogen, Waltham, MA,

USA). cDNA was extracted using SureScript™ First-Strand cDNA Synthesis Kit (GeneCopoeia, Guangzhou, China). mRNAs amplification was performed using the following specific primers: HO-1 (102 bp) forward 5'-CCATCCCTTACACACCAGCC-3', reverse 5'-GGTAGCGGGTATATGCGTGG-3'; β -tubulin (152 bp) forward 5'-GAGGCAGATGGCAGTGACAG-3', reverse 5'-TGGTTGGGGAACACGGAGTA-3' (Sangon Biotech, Shanghai, China).

2.10 Statistical Analysis

Quantitative data are presented as mean \pm standard error. Measurement data were presented as $\bar{x} \pm s$. Multiple groups of measurement data were compared using a single-factor analysis of variance and an advanced homogeneity of variance test. In the case of uniform distribution, the least significant difference test was used, and in the case of skewed distribution, Dunnett's T3 test was used. Survival and statistical data were assessed using Kaplan–Meier analysis. Differences were considered statistically significant when $p < 0.05$. All statistical graphs were created using the GraphPad Prism software (GraphPad Software 9, Inc., San Diego, CA, USA), and all data were analyzed using SPSS 24.0 (IBM Corp., Armonk, NY, USA).

3. Results

3.1 Fluorescence Results and HO-1 Expression Level in Liver Tissue after AAV Transduction

The fluorescence intensity in the liver tissue was assessed 21 days after AAV transduction (Fig. 1A–D). HO-1 transcription levels were significantly lower in the shRNA-HO-1 group than in the shRNA-NC group. The gene transcription level was higher in the AAV-HO-1 group than in the AAV-NC (normal control), shRNA-HO-1, shRNA-NC, and normal groups (Fig. 1E). The fluorescence intensity and HO-1 mRNA transcription levels in the four DCD groups are shown in Table 1 and at four-time points are shown in Table 2.

3.2 HO-1 Expression Significantly Affected Survival Curve Following LT

The overall comparison result was $\chi^2 = 14.449$ (degree of freedom $\nu = 5$; $p < 0.05$). In addition, paired comparisons revealed significant survival ($p < 0.05$) among the sham, DCD + shRNA-HO-1, and DCD + AAV-HO-1 groups (Fig. 1F).

3.3 HE Staining Score of Liver Tissues at Different Reperfusion Time Points

The effects of ischemia on the transplanted liver were assessed at different durations of reperfusion (DCD + IR6h, DCD + IR24h, DCD + IR72h, and DCD + IR168h groups). HE staining revealed rapid progression of tissue damage in the DCD + IR6h group, along with obvious necrosis. In the DCD + IR24h group, the liver tissue damage was greater

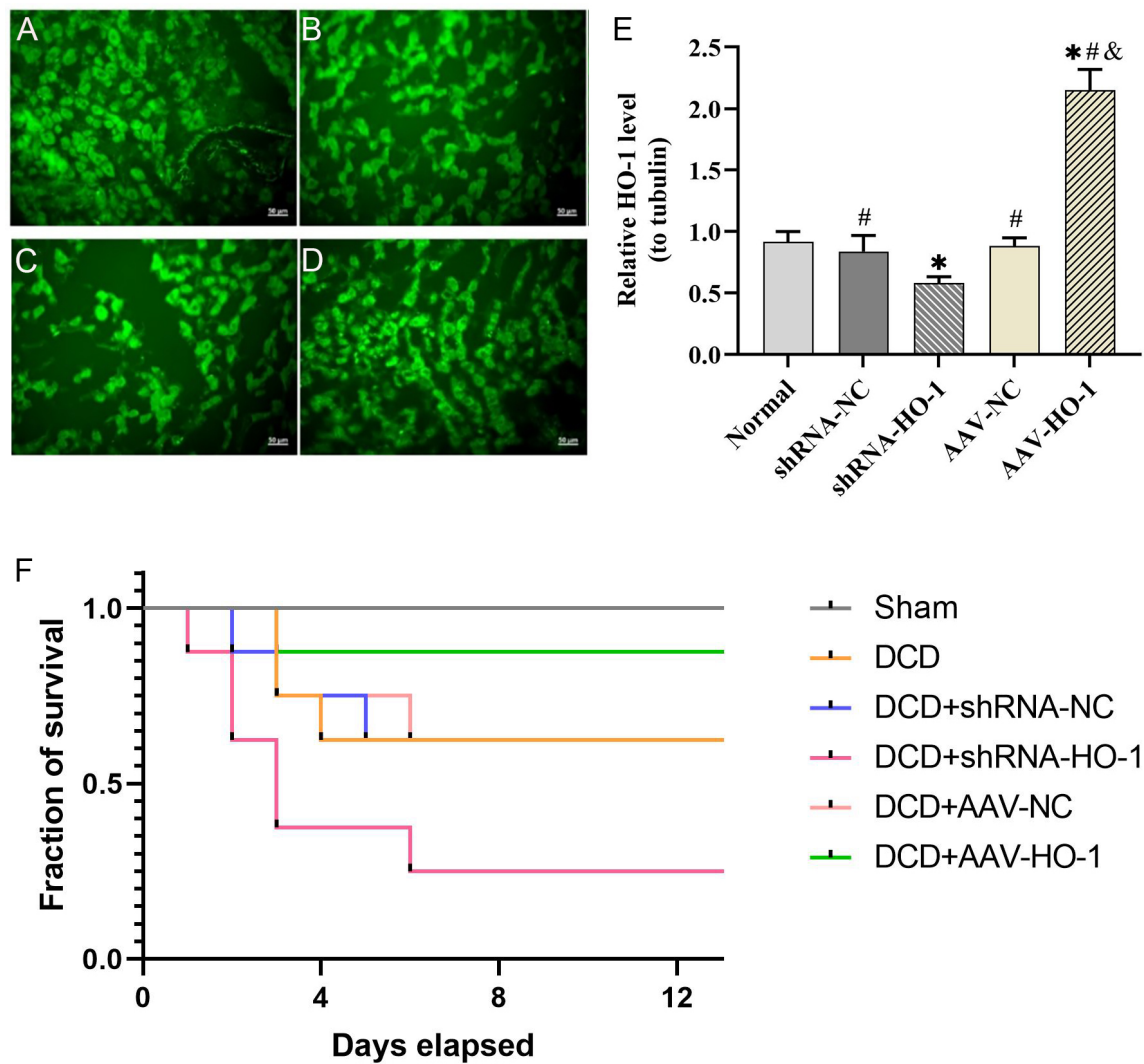


Fig. 1. Efficiency of AAV transfection and HO-1 mRNA transcription level in rat liver tissue. (A) AAV2/9-EGFP interference control. 400 \times . (B) AAV2/9-r-Hmox1 shRNA-EGFP interferes with expression. 400 \times . (C) AAV2/9-ZsGreen overexpression control. 400 \times . (D) AAV2/9-CMV-r-Hmox1-3xflag-ZsGreen is overexpressed. 400 \times . (E) The change in *HO-1* gene transcription level mRNA after AAV transfection in SD rats. *, compared with the normal group, the difference is statistically significant, $p < 0.05$; #, compared with the shRNA-HO-1 group, the difference is statistically significant, $p < 0.05$; &, compared with the AAV-NC group, the difference is statistically significant, $p < 0.05$. (F) Analysis of postoperative survival time of SD rats between groups after successful DCD liver transplantation modeling. AAV, adenoassociated virus; HO-1, Heme oxygenase-1; DCD, Donors after circulatory death; shRNA, short hairpin RNA; NC, normal control.

than in the DCD + IR6h group, with extensive necrosis. However, in the DCD + IR72h and DCD + IR168h groups, necrosis was not as obvious as in the DCD + IR24h group, and the degree of damage gradually decreased. Particularly, the normal lobules had been destructured, and the sinus space was still wider than normal. Compared with the normal group, the DCD + IR6h, DCD + IR24h, DCD + IR72h, and DCD + IR168h groups demonstrated significantly greater liver tissue damage ($p < 0.05$). Compared with the DCD + IR6h group, the normal, DCD + IR24h, and DCD + IR168h groups showed significant differences in the degree of injury ($p < 0.05$) (Fig. 2).

3.4 ROS Levels in Reperfused Liver Tissue after DCD LT

Over time, the ROS levels in the liver tissues of each group decreased after reperfusion. Compared with the normal group, the DCD + IR6h, DCD + IR24h, DCD + IR72h, and DCD + IR168h groups had significantly lower ROS levels ($p < 0.05$). Compared with the DCD + IR6h group, the normal, DCD + IR72h, and DCD + IR168h groups were significantly different ($p < 0.05$) (Fig. 3).

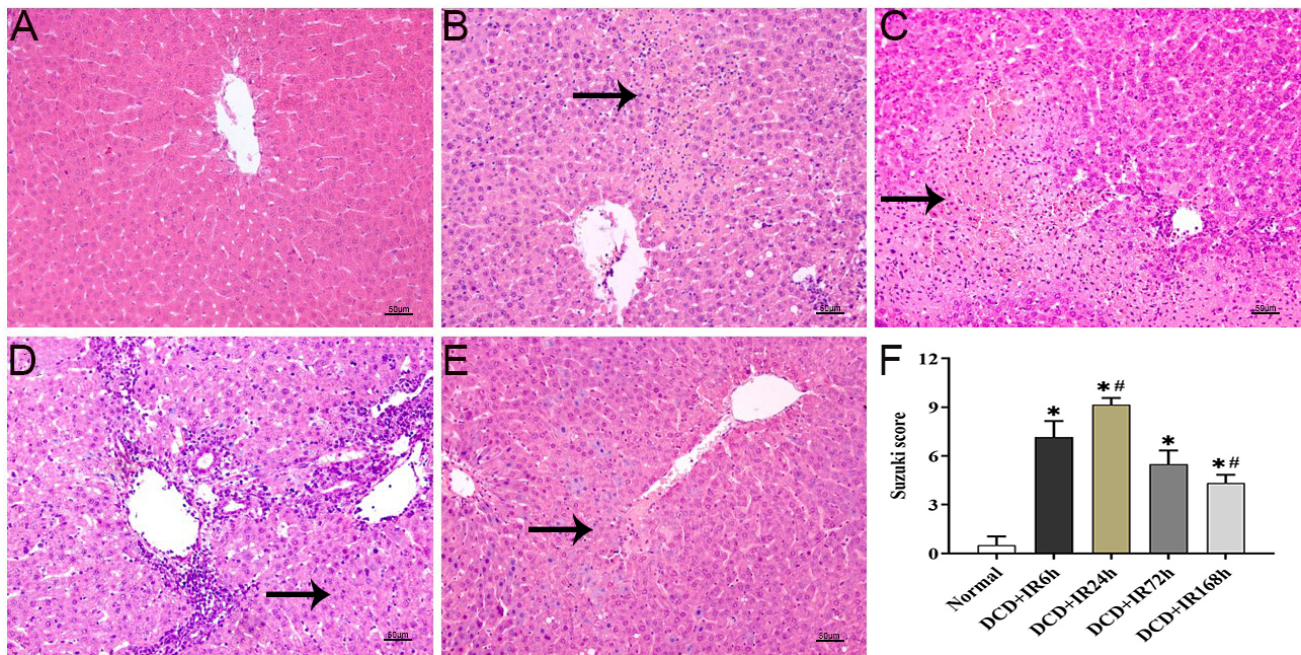


Fig. 2. HE staining and Suzuki score of the donor livers after liver transplantation. (A–E) HE results of liver tissue after LT, (A) normal, (B) DCD + IR6h, (C) DCD + IR24h, (D) DCD + IR72h, and (E) DCD + IR168h. (F) The histogram based on the Suzuki score, *, $p < 0.05$ compared with normal; #, $p < 0.05$ compared with DCD + IR6h. LT, liver transplantation; IR, ischemia-reperfusion.

Table 1. DCD groups of study of biomarkers after reperfusion.

Characteristic	DCD + shRNA-NC	DCD + shRNA-HO-1	DCD + AAV-NC	DCD + AAV-HO-1
HO-1	↑/#	↓	↑/#	↑/*#&
p22	↑/#	↑/*	↑/#	↓/#&
cleaved-N-GSDMD	↑/#	↑/*	↑/#	↓/#&
NLRP3	↑/#&	↓/*	↓/#	↓/*&
ROS	↑/#	↑/*	↑/#	↓/*#&
ALT	↑/#	↑/*	↑/#	↓/*#&
AST	↑/#	↑/*	↑/#	↓/*#&
IL-1 β	↑/#	↑/*	↑/#	↓/*#&
IL-18	↑/#	↑/*	↑/#	↓/*#&

*, compared with DCD group, $p < 0.05$; #, compared with DCD + shRNA-HO-1 group, $p < 0.05$; &, compared with DCD + AAV-NC group, $p < 0.05$; ↑/↓, compared with DCD group. ALT, alanine transaminase; AST, aspartate aminotransferase; IL, interleukin; ROS, reactive oxygen species; GSDMD, gasdermin D.

3.5 Change in Liver Function and Cytokines after LT

The liver function and cytokine levels would change accordingly after reperfusion. The results revealed that ALT and AST levels increased significantly at 6 and 24 h but decreased at 72 and 168 h. Compared with the normal group, ALT and AST levels were significantly different in the DCD + IR6h, DCD + IR24h, DCD + IR72h, and DCD + IR168h groups ($p < 0.05$). The normal, DCD + IR72h, and DCD + IR168h groups differed significantly from the DCD + IR6h group ($p < 0.05$) (Fig. 4A,B).

Over time, IL-1 β and IL-18 levels in the liver tissues increased and then decreased, which was consistent. Compared with those in the normal group, cytokine levels were significantly different in the DCD + IR6h, DCD

+ IR24h, DCD + IR72h, and DCD + IR168h groups ($p < 0.05$). Moreover, the normal, DCD + IR72h, and DCD + IR168h groups differed significantly from the DCD + IR6h group ($p < 0.05$) (Fig. 4C,D).

3.6 The Expression of Each Protein was Detected in Tissue

Over time, proteins showed a trend with the prolongation of the postoperative reperfusion time after LT. Results of western blotting revealed that (Fig. 4E) HO-1 expression was significantly increased in the DCD + IR6h group, but it decreased in the other long-term groups. Moreover, HO-1 expression in the DCD + IR6h group was significantly different from the normal group, DCD + IR72h, and DCD + IR168h groups ($p < 0.05$). However, it was not significantly different from the DCD + IR24h group. In addition,

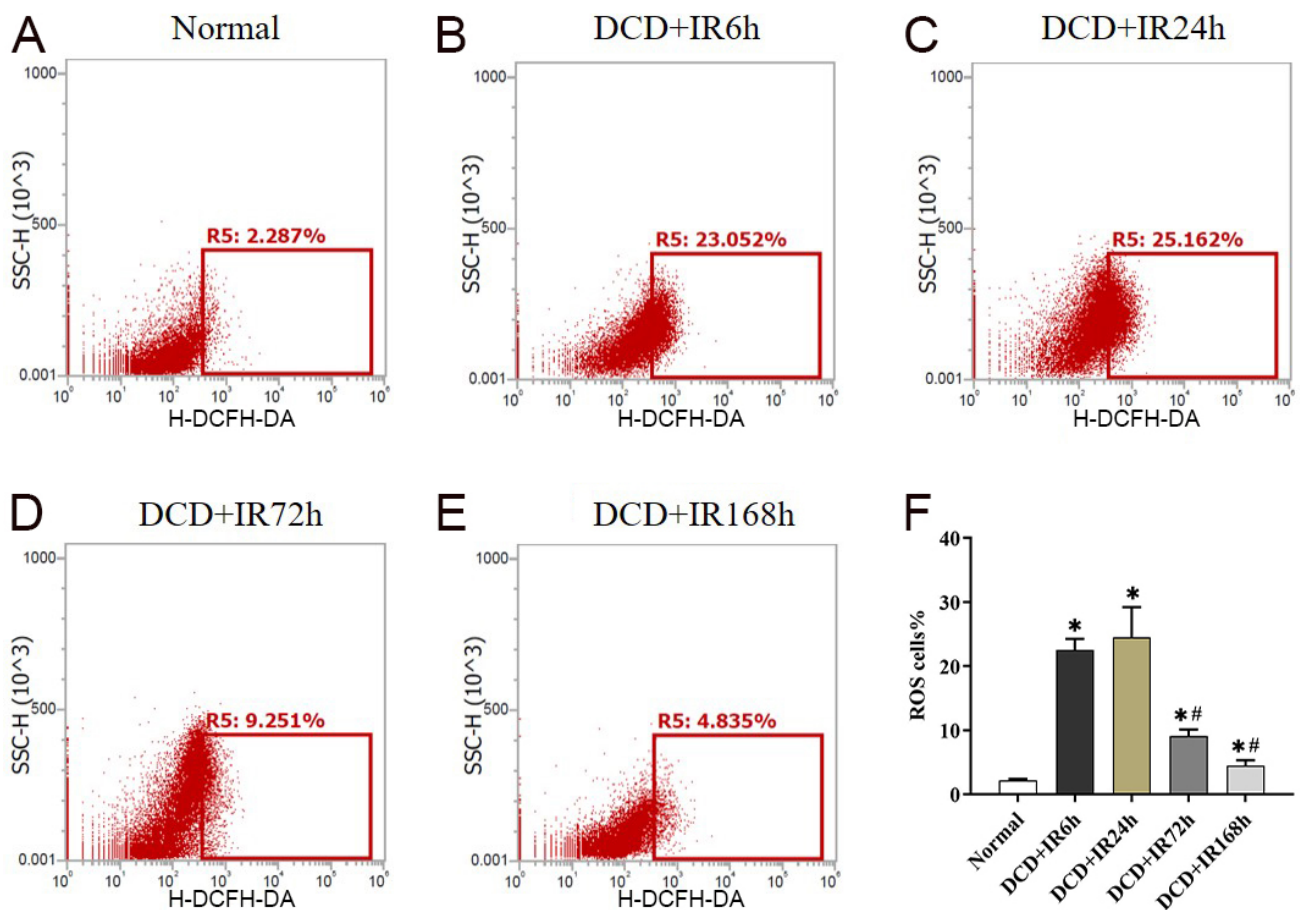


Fig. 3. ROS level changes after LT. (A–E) After DCD LT, the donor liver of ischemia was followed by different durations of reperfusion for 6 h, 24 h, 72 h, and 168 h. (F) Flow cytometry was used to detect the expression level of ROS in the liver tissue. *, compared with normal group, $p < 0.05$; #, compared with DCD + IR6h group, $p < 0.05$.

Table 2. DCD, expression of biomarkers at various time points after reperfusion.

Characteristic	6 h	24 h	72 h	168 h
HO-1	↑/*	↑/*	↑/*#	↑/#
p22	↑/*	↑/*	↑/*#	↑/#
cleaved-N-GSDMD	↑/*	↑/*	↑/*#	↑/#
NLRP3	↑/*	↑/*#	↑/*#	↑/*#
ROS	↑/*	↑/*	↑/*#	↑/*#
ALT	↑/*	↑/*	↑/*#	↑/*#
AST	↑/*	↑/*	↑/*#	↑/*#
IL-1 β	↑/*	↑/*	↑/*#	↑/*#
IL-18	↑/*	↑/*	↑/*#	↑/*#

*, compared with normal group, $p < 0.05$; #, compared with DCD + IR6h group, $p < 0.05$; ↑ compared with normal group.

compared with the normal group, the DCD + IR6h, DCD + IR24h, and DCD + IR72h groups had significantly different HO-1 expression ($p < 0.05$) (Fig. 4F).

The p22 of pro-caspase1 was significantly increased in the short term but gradually decreased over the long term. Compared with the normal group, p22 expression in the

DCD + IR6h, DCD + IR24h, and DCD + IR72h groups was significantly different ($p < 0.05$). Although p22 expression in the DCD + IR168h group was higher than the normal group, the difference was not statistically significant. Compared with the DCD + IR6h group, p22 expression in the normal, DCD + IR72h, and DCD + IR168h groups was statistically different ($p < 0.05$) (Fig. 4G).

The expression of cleaved-N-GSDMD was the highest in the short-term groups but decreased in the long-term groups. Compared with the normal group, the expression of cleaved-N-GSDMD in the DCD + IR6h, DCD + IR24h, and DCD + IR72h groups were significantly different ($p < 0.05$). Although the expression in the DCD + IR168h group was higher than in the normal group, it was not statistically significant. Compared with the DCD + IR6h group, the normal, DCD + IR72h, and DCD + IR168h had significantly different expression levels ($p < 0.05$) (Fig. 4H).

Immunohistochemistry revealed that NLRP3 was not expressed in the normal group. Notably, the DCD + IR6h and DCD + IR24h groups demonstrated extensive necrosis. However, NLRP3 expression in the DCD + IR6h group was the lowest among the other groups. Over time, NLRP3

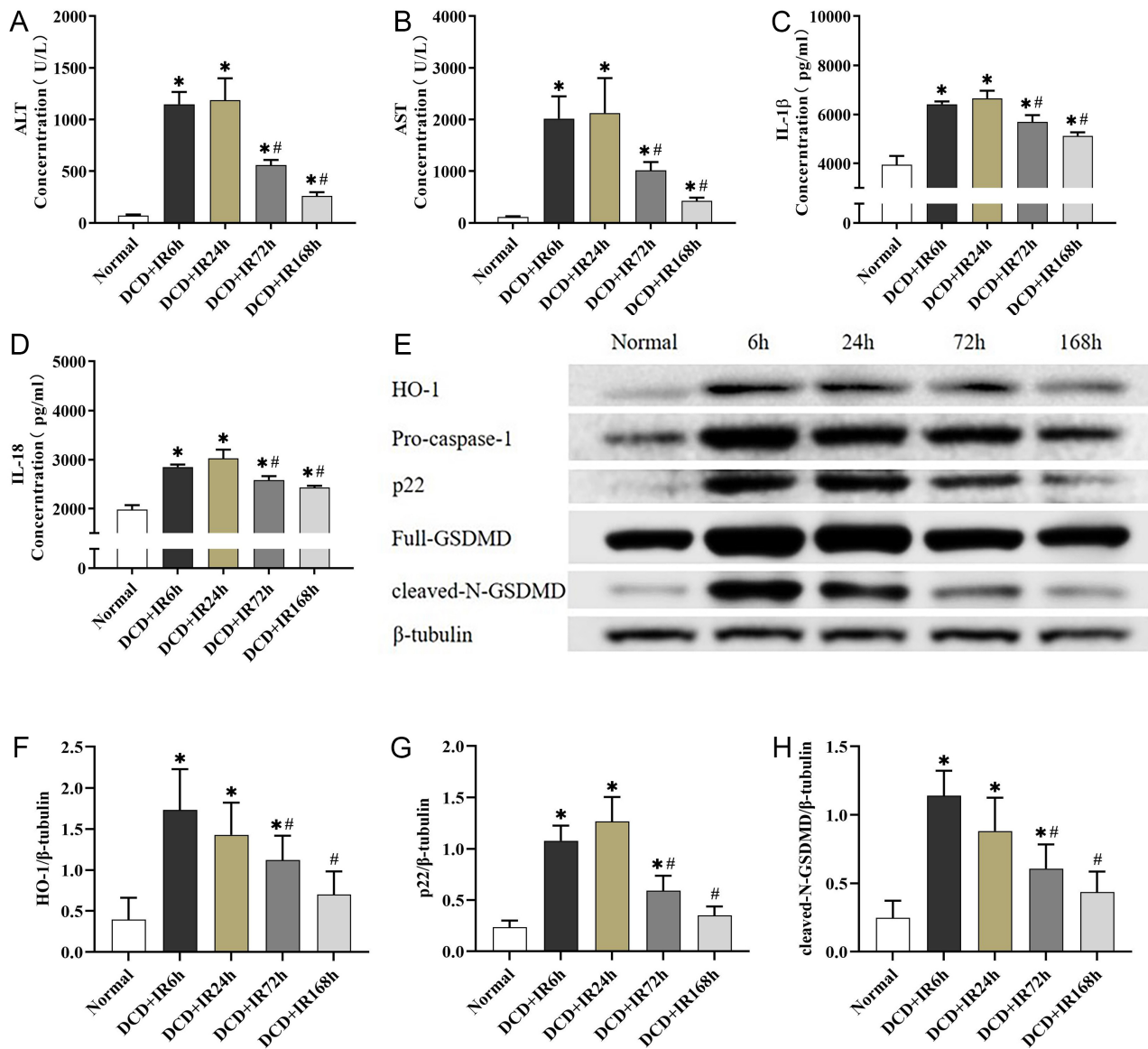


Fig. 4. Liver function and protein changes after LT. (A) Biochemical analysis results of ALT. (B) Biochemical analysis results of AST. (C) The level of IL-1 β in serum. (D) The level of IL-18 in serum. (E) Western blot method to detect the protein expression of HO-1, Caspase-1, p22, full-GSDMD, and cleaved-N-GSDMD in each group. (F–H) the statistical results of HO-1/ β -tubulin, p22/ β -tubulin, and cleaved-N-GSDMD/ β -tubulin in each group, respectively. *, compared with normal, $p < 0.05$; #, compared with DCD + IR6h, $p < 0.05$.

expression increased in the short term but decreased over the long term. Compared with the DCD + IR6h group, the normal group, DCD + IR24h, DCD + IR72h, and DCD + IR168h groups differed significantly in terms of NLRP3 expression ($p < 0.05$) (Fig. 5).

3.7 Following AAV Treatment, the Donor Liver of DCD LT with IRI for Reperfusion of Tissues with HE Results and Suzuki Score

Based on previous experiments, the time point of reperfusion was chosen as 6 h in this study. After 21 days of AAV pretreatment, the donor's liver was reperused for

6 h after DCD LT. Compared with the control group, the DCD + shRNA-HO-1 group exhibited greater damage in the liver tissue, with larger areas of necrosis, severe congestion, and sinus space. The necrotic area in the DCD + AAV-HO-1 group was significantly reduced, the hepatic cord was intact, the sinus space was approximately the same as the sham group, and the degree of congestion was significantly lower. Compared with the DCD group, the sham, DCD + shRNA-HO-1, and DCD + AAV-HO-1 groups showed statistically significant differences in the degree of damage ($p < 0.05$). The damage was not significantly different in the DCD + shRNA-NC and DCD + AAV-NC groups. More-

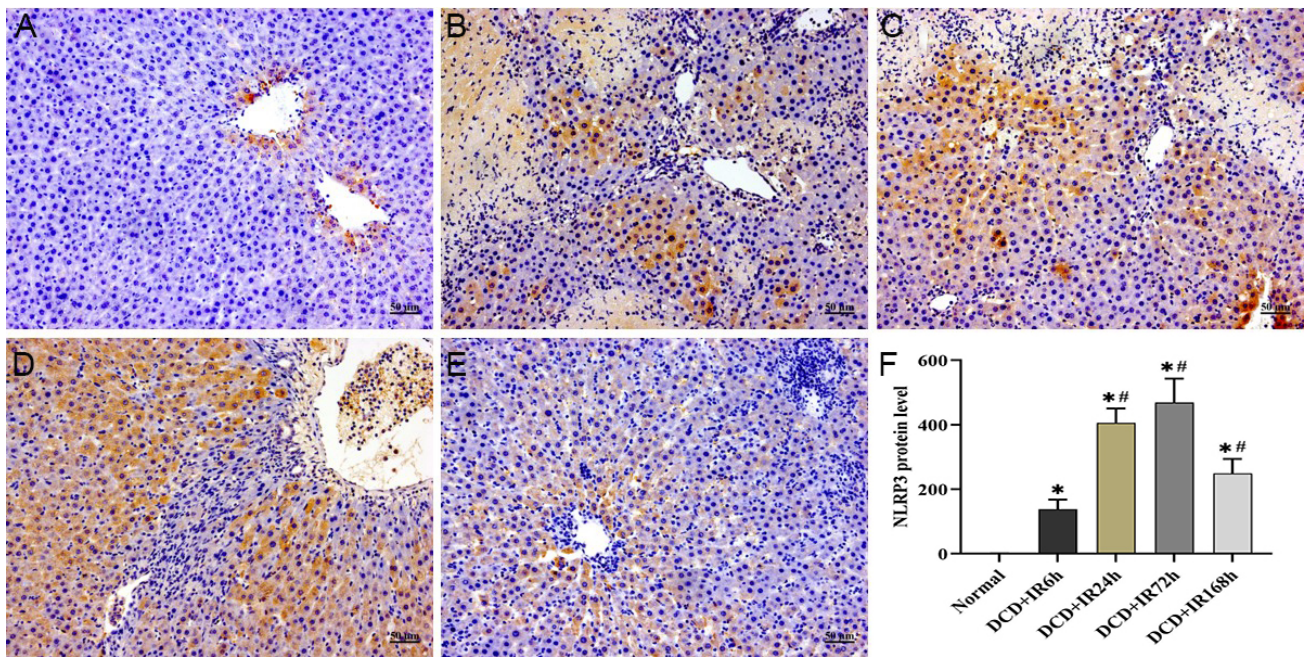


Fig. 5. Change in NLRP3 after LT. (A–E) Immunohistochemistry of NLRP3 results of liver tissue after LT. (A) Normal, (B) DCD + IR6h, (C) DCD + IR24h, (D) DCD + IR72h and (E) DCD + IR168h. (F) The expression level of NLRP3 in the liver tissue. *, compared with normal, $p < 0.05$; #, compared with DCD + IR6h, $p < 0.05$.

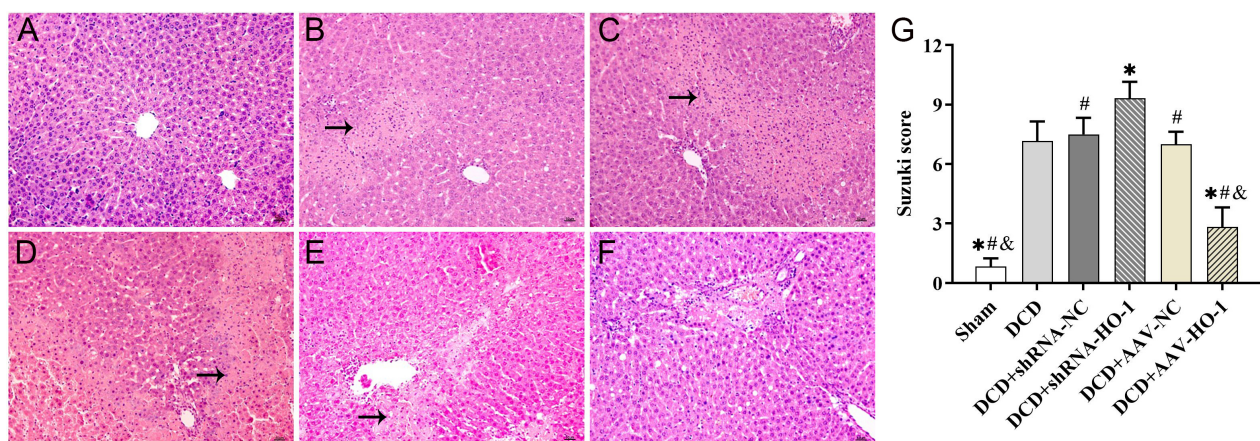


Fig. 6. HE staining results and Suzuki score of different groups after AAV pretreatment. (A–F) Postoperative liver tissue HE staining results. (A) Sham, (B) DCD, (C) DCD + shRNA-NC, (D) DCD + shRNA-HO-1, (E) DCD + AAV-NC, and (F) DCD + AAV-HO-1. (G) A histogram based on the Suzuki score. *, compared with the DCD group, $p < 0.05$; #, compared with the DCD + shRNA-HO-1 group, $p < 0.05$; &, compared with the DCD + AAV-NC group, $p < 0.05$.

over, compared with the degree of damage in the DCD + shRNA-HO-1 group, the DCD, DCD + shRNA-NC, DCD + AAV-NC, and DCD + AAV-HO-1 groups was statistically significant ($p < 0.05$). In addition, the DCD + AAV-NC and DCD + AAV-HO-1 groups differed significantly in the degree of damage ($p < 0.05$) (Fig. 6).

3.8 ROS Level Following AAV Treatment

The hepatic ROS level in the DCD + shRNA-HO-1 group was significantly higher than that in other groups but was significantly lower than the DCD + AAV-HO-1

group. The ROS level differed significantly between the DCD + shRNA-HO-1 group and the DCD, DCD + shRNA-NC, DCD + AAV-NC, and DCD + AAV-HO-1 groups ($p < 0.05$). Similarly, the DCD + AAV-NC and DCD + AAV-HO-1 groups had significantly different ROS levels ($p < 0.05$) (Fig. 7).

3.9 Changes in Liver Function and Cytokine Levels Following AAV Treatment

Following DCD LT, the donor liver was pretreated with AAV for 21 days and was then reperused for 6 h.

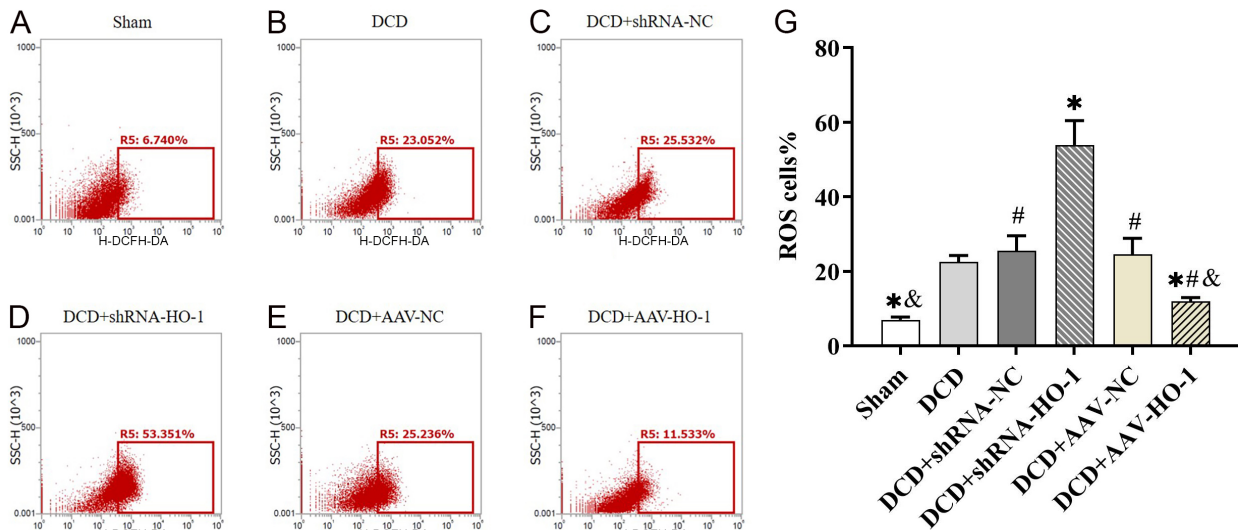


Fig. 7. After AAV pretreatment, the donor's liver was reperused for 6 h after DCD LT and the level of ROS was measured in liver tissues. *, compared with DCD group, $p < 0.05$; #, compared with DCD + shRNA-HO-1 group, $p < 0.05$; &, compared with DCD + AAV-NC group, $p < 0.05$. (A–F) The result of ROS level in flow cytometry. (A) Sham; (B) DCD; (C) DCD + shRNA-NC; (D) DCD + shRNA-HO-1; (E) DCD + AAV-NC, (F) DCD + AAV-HO-1 groups. (G) The bar chart shown the percentage of ROS cells in each group.

Following this, serum ALT and AST levels in the DCD + shRNA-HO-1 group increased significantly. However, these levels in the DCD + AAV-HO-1 group showed a downward trend compared with those in the control, but they were still higher than those in the sham group.

Compared with the DCD + shRNA-HO-1 group, the DCD, DCD + shRNA-NC, DCD + AAV-NC, and DCD + AAV-HO-1 groups had significantly different ALT levels ($p < 0.05$). Moreover, the ALT level differed significantly between the DCD + AAV-NC and DCD + AAV-HO-1 groups ($p < 0.05$) (Fig. 8A).

Compared with the DCD + shRNA-HO-1 group, the DCD, DCD + shRNA-NC, DCD + AAV-NC, and DCD + AAV-HO-1 groups had significantly different AST levels ($p < 0.05$). Moreover, the AST level differed significantly between the DCD + AAV-NC and DCD + AAV-HO-1 levels ($p < 0.05$) (Fig. 8B).

The hepatic levels of IL-1 β and IL-18 in the DCD + shRNA-HO-1 group were higher than in the other groups. However, in the DCD + AAV-HO-1 group, the hepatic IL-1 β and IL-18 levels showed a downward trend compared with the control group, were significantly lower than those in the DCD + shRNA-HO-1 group, and were slightly higher than those in the sham group. Moreover, the levels of IL-1 β and IL-18 in each group correlated positively.

Compared with the DCD + shRNA-HO-1 group, the IL-1 β level differed significantly in the DCD, DCD + shRNA-NC, DCD + AAV-NC, and DCD + AAV-HO-1 groups ($p < 0.05$). Compared with the DCD + AAV-NC group, the IL-1 β level in the sham and DCD + AAV-HO-1 groups was significantly different ($p < 0.05$) (Fig. 8C).

Compared with the IL-18 level in the DCD + shRNA-HO-1 group, the DCD, DCD + shRNA-NC, DCD + AAV-NC, and DCD + AAV-HO-1 groups was significantly different ($p < 0.05$). Compared with the DCD + AAV-NC group, the sham and DCD + AAV-HO-1 groups had significantly different IL-18 levels ($p < 0.05$) (Fig. 8D).

3.10 Protein Expression Following AAV Treatment

The HO-1 mRNA level in the transplanted liver in each group was in line with our expectations. The mRNA transcription level of the HO-1 interference expression group was significantly lower than that of the control but was slightly higher than that of the sham group. In contrast, the mRNA transcription level of the DCD + AAV-HO-1 was significantly higher. The mRNA transcription levels in the DCD, DCD + shRNA-NC, DCD + shRNA-HO-1, DCD + AAV-NC, and DCD + AAV-HO-1 groups were significantly different ($p < 0.05$). Moreover, at the protein level, the trend in HO-1 expression was consistent with that at the transcription level. HO-1 expression was significantly different between the DCD + shRNA-HO-1 group and all other groups except for DCD ($p < 0.05$). At the same time, HO-1 expression was significantly different between the DCD + AAV-HO-1 and DCD + AAV-NC groups ($p < 0.05$) (Fig. 8E–G).

The expression of p22 of pro-caspase1 was increased significantly in the DCD + shRNA-HO-1 group but was decreased in the DCD + AAV-HO-1 group. In addition, the expression was significantly different in the DCD + shRNA-HO-1 group compared with the DCD, DCD + shRNA-NC, DCD + AAV-NC, and DCD + AAV-HO-1 groups ($p < 0.05$).

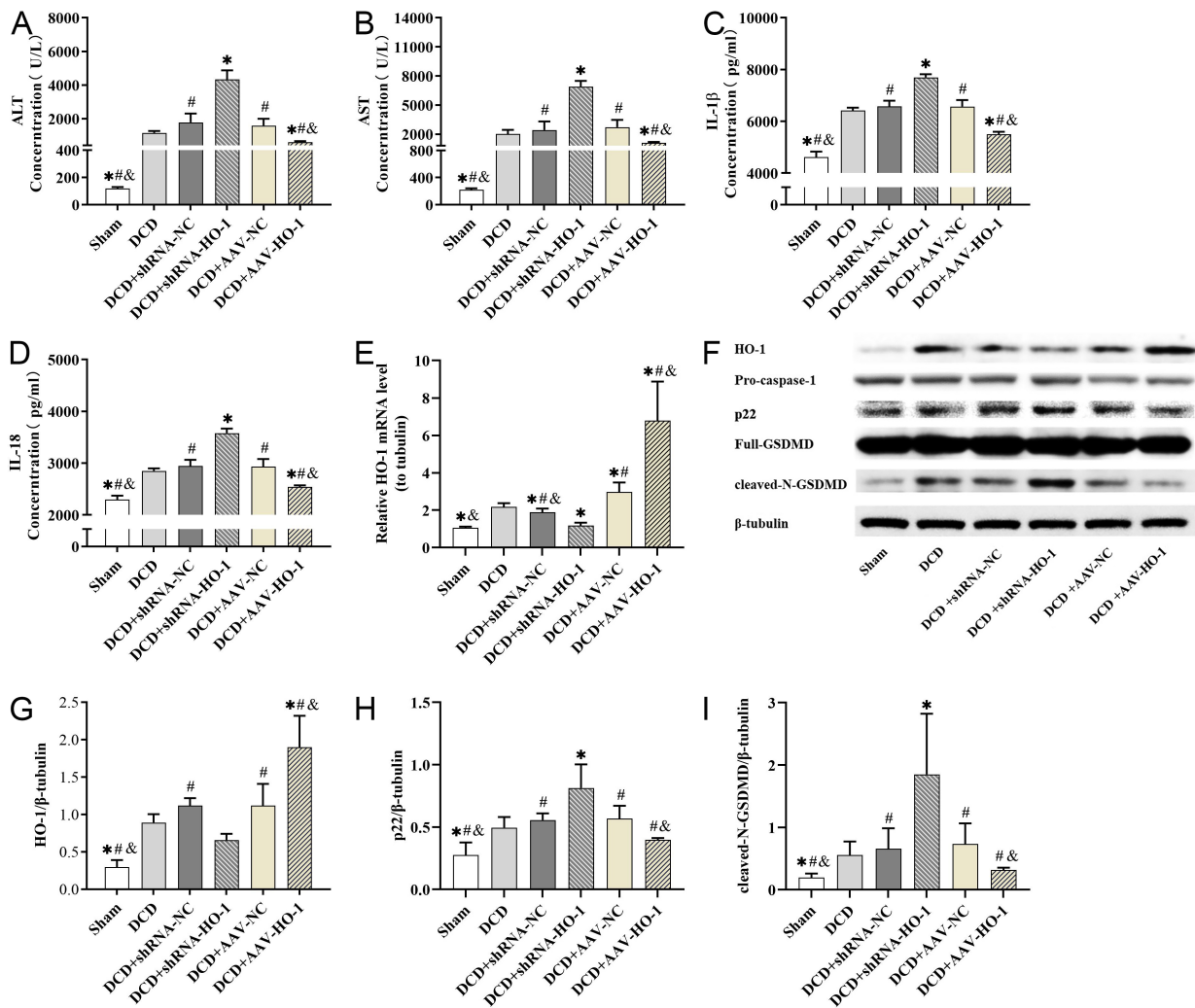


Fig. 8. With AAV pretreatment, the donor liver was reperused for 6 hours after DCD LT. (A) Biochemical analysis results of ALT. (B) Biochemical analysis results of AST. (C) The expression level of IL-1 β in serum. (D) The expression level of IL-18 in serum. (E) The mRNA level of HO-1 in the liver tissue. (F) Western blot method to detect the protein expression of HO-1, Caspase-1, p22, full-GSDMD, and cleaved-N-GSDMD in each group. (G) Statistical results of (G) HO-1/ β -tubulin, (H) p22/ β -tubulin, and (I) cleaved-N-GSDMD/ β -tubulin in each group. *, compared with DCD group, $p < 0.05$; #, compared with DCD + shRNA-HO-1 group, $p < 0.05$; &, compared with DCD + AAV-NC group, $p < 0.05$.

0.05). Moreover, the DCD + AAV-NC and DCD + AAV-HO-1 groups differed significantly in terms of p22 expression ($p < 0.05$) (Fig. 8H).

The trend in the expression of spliced cleaved-N-GSDMD of full-GSDMD was similar to that of p22. The expression of spliced cleaved-N-GSDMD was increased significantly in the DCD + shRNA-HO-1 group and was decreased significantly in the DCD + AAV-HO-1 group. Compared with spliced cleaved-N-GSDMD expression in the DCD + shRNA-HO-1 group, the DCD, DCD + shRNA-NC, DCD + AAV-NC, and DCD + AAV-HO-1 groups was significantly different ($p < 0.05$) (Fig. 8I).

In addition, treatment altering the expression of HO-1 immediately affected the NLRP3 level, which in turn affected the level and activation of caspase-1 and GSDMD.

Immunohistochemical analysis revealed that NLRP3 expression in the DCD + shRNA-HO-1 group was significantly decreased; the group also had large areas of tissue necrosis. The expression differed significantly among DCD, DCD + shRNA-NC, and DCD + AAV-NC groups ($p < 0.05$). Compared with the DCD + AAV-NC group, the DCD + AAV-HO-1 group had significantly lower NLRP3 expression ($p < 0.05$) (Fig. 9).

4. Discussion

LT is reportedly the most effective curative treatment for end-stage liver disease [22]. However, in cases of DCD, it is essential to optimize graft function and reduce IRI to eventually increase donor liver availability [23]. HO-1 is the rate-limiting enzyme of heme metabolism, and its high

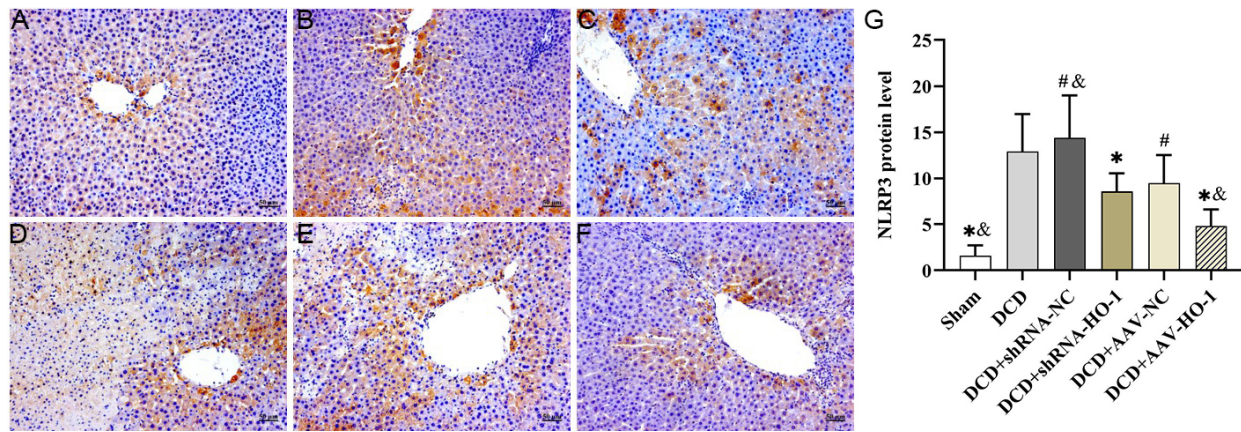


Fig. 9. Following AAV pretreatment, the donor liver was reperused for 6 hours after DCD LT, and the expression of NLRP3 was observed. (A–F) Immunohistochemistry results of NLRP3 coloration in each group (200 \times). (A) Sham, (B) DCD, (C) DCD + shRNA-NC, (D) DCD + shRNA-HO-1, (E) DCD + AAV-NC, and (F) DCD + AAV-HO-1. (G) The statistical results of the relative expression levels of NLRP3 in each group relative to the sham. *, compared with DCD group, $p < 0.05$; #, compared with DCD + shRNA-HO-1 group, $p < 0.05$; &, compared with DCD + AAV-NC group, $p < 0.05$.

expression is currently recognized as a key cytoprotective mechanism against inflammation, hyperthermia, and IRI [24]. In LT involving DCD, the expression of HO-1 was correlated with the ischemia-reperfusion time. Moreover, HO-1 expression increased significantly in the DCD + IR6h group and gradually decreased. This trend coincided with the most severe early stress response of IRI, which additionally correlated with the ROS level. These findings are consistent with those of previous studies [10]. In the present study, HO-1 expression was significantly increased at 6 h and 24 h, indicating that DCD significantly induces HO-1 expression after IRI, which may have the potential to resist oxidative stress damage. However, the recent high expression of HO-1 did not immediately relieve liver damage. As shown in Fig. 2, HE staining revealed extensive necrosis in the DCD + IR6h group, with the most severe damage being observed in the DCD + IR24h group. According to the Suzuki score, damage at 78 and 168 h was significantly lower than at 6 and 24 h. In addition, serum ALT and AST levels indicated that liver damage in the early stages was severe, with that at 24 h being slightly lower than at 6 h, which then decreased gradually. We speculate in the early stages, although HO-1 was highly expressed during IRI and LT, liver damage occurred before this expression. Therefore, high HO-1 expression could only be seen as a follow-up response to oxidative stress and could play a role in anti-inflammatory and anti-injury effects in the future. The gradual reduction in the long-term damage may be because the high expression of HO-1 in the early stage exerted a long-term effect, which enhanced the tolerance of the undamaged liver tissue to oxidative stress and inhibited the combination of DAMPs and PRR. This subsequently inhibited the inflammatory response and reduced the long-term damage to liver cells, which was consistent with previous findings [14].

To further explain the cause of hepatic injury, we tested the level of NLRP3, cleaved caspase-1 (p22/p20), and cleaved N-GSDMD in the donor's liver at each IRI time point. The results showed that the expression of p22 and cleaved N-GSDMD was the highest at 6 and 24 h, indicating that pyroptosis occurred when the donor's liver underwent IRI. The degree of pyroptosis was the highest at the beginning of IRI and gradually reduced. However, NLRP3, which is directly related to pro-caspase-1 activation, was found to have the opposite effect. In addition, immunohistochemistry results revealed that the NLRP3 level in the IR6h group was the lowest, inconsistent with the most severe scorch death in the IR6h group. Burdette *et al.* [25] have revealed that NLRP3 is expressed in the cytoplasm and mediates pro-caspase-1 splicing activation and functioning. Therefore, we speculated that the inconsistent expression trend of NLRP3 was due to severe liver damage in the IR6h group. After cell rupture, NLRP3 is completely released and cannot be assessed by immunohistochemistry. This speculation was consistent with the most severe pyroptosis observed in the IR6h group.

We additionally tested IL-1 β and IL-18 levels in the liver tissues and found that the levels were the highest at 24 h and decreased gradually after that. Zhang *et al.* [26] revealed that warm ischemia injury could lead to a decrease in the number of KCs in the liver, resulting in a general decrease in Th1 cytokines produced by hepatic non-parenchymal cells. However, postoperative ischemia-reperfusion localizes local inflammatory chemokines from the transplanted liver to other body parts. These chemokines include CXCL1, CXCL2, and CXCL8 to attract neutrophil infiltration and CCL1, CCL2, CCL25, and CX3CL1 to chemoattract bone marrow mononuclear cell infiltration [27]. In the present study, HE staining revealed that the number of inflammatory cells that infiltrated

the liver tissue in the IR24h group was significantly higher than in the IR6h group, which could explain the upward trend of IL-1 β and IL-18 levels.

RT-qPCR detected the overexpression of HO-1, HO-1 shRNA recombinant AAV and the respective blank control viral vectors were transduced into normal SD rats. This showed that the intervention effect of HO-1 overexpression and HO-1 shRNA recombinant AAV was statistically significant compared with no intervention in the blank group. HO-1 overexpression was positively correlated with the survival of SD rats after DCD LT.

RT-qPCR and western blotting revealed that the expression of HO-1 was in line with expectations. When HO-1 was overexpressed, the expression of p22 and cleaved N-GSDMD was significantly downregulated. However, when HO-1 expression was downregulated, the levels of p22 and cleaved N-GSDMD increased significantly. GSDMD-N and -C mediate cell perforation and rupture causes caspase-1-dependent cell pyroptosis [9]. Accordingly, under high HO-1 expression in the donor's liver, pyroptosis was inhibited when the DCD underwent ischemia-reperfusion after LT. This result was consistent with the results of HE staining of the transplanted liver. In addition, HE staining showed that when HO-1 was overexpressed, tissue cell damage was minimal, with mild cell destruction and lysis. However, inhibition of HO-1 expression resulted in aggravation of liver cell damage and the necrotic area compared with the control conditions. In addition, cell lysis was severe, with no intact and normal hepatic cord or hepatic sinusoid structure. According to AST and ALT levels, the overexpression of HO-1 could reduce the level of liver damage after LT from DCD. This proves that the degree of damage after LT was significantly alleviated by HO-1 overexpression in the donors. In addition, when HO-1 expression was inhibited, NLRP3 levels were significantly lower than in the donor's liver with HO-1 overexpression. This effect could be attributed to severe liver tissue necrosis observed when HO-1 expression is inhibited, which decreases immunohistochemical detection of NLRP3. Regarding the HO-1 overexpression group, as the tissue structure was intact and immunohistochemical results were normal, these data are reliable. Compared with the control group, it was significantly lower, indicating that NLRP3 activation was inhibited at that time.

In the early stage of IRI after LT, HO-1 expression was increased, but this was only a follow-up response to oxidative stress and could not immediately alleviate liver injury. However, the early-stage high expression of HO-1 played a role in the recovery of long-term liver function. In the IR6h group, oxidative stress was the most severe among all groups, and early pyroptosis was likely to be one of the main causes of liver damage. Therefore, inhibiting early liver injury could be the key to promoting the recovery of liver function after transplant.

Survival analysis revealed significant differences in at least two groups. Subsequent pairwise comparisons demonstrated that the sham (14.00 ± 0.00), DCD + shRNA-HO-1 (5.63 ± 5.37), and the DCD + AAV-HO-1 (12.63 ± 3.89) groups were significantly different ($p < 0.05$). In addition, the survival rate among the DCD, DCD + shRNA-NC, and DCD + AAV-NC was not significantly different. Compared with the survival rate of the sham group, that of the DCD group decreased from 100% to 75%. Although this was not significant, it proved the success of the LT model. For SD rats with HO-1 overexpression and AAV pretreatment (which downregulates HO-1 expression), short-term survival rates after orthotopic LT were 87.5% and 37.5%, respectively. This indicated that blocking HO-1 expression in the liver did not inhibit the damage caused by warm ischemia for 10 min and IRI in the transplanted liver. Thus, the ability of the liver to tolerate stress response was reduced. However, compared with HO-1 interference-expressed cadaveric liver, the survival rate of HO-1 overexpressed cadaveric liver after LT was higher, which proved that HO-1 overexpression could significantly increase survival after LT. Therefore, these results suggest that HO-1 may play an important role in protecting the quality of cadaveric livers from DCD, and preconditioning donor's livers and ensuring high HO-1 expression in donor livers may increase survival rate after cadaveric surgery. In the present study, the donor underwent pretreatment for inducing HO-1 overexpression and HO-1 shRNA recombinant AAV therefore it was able to reach a state of stable HO-1 expression before LT. This proved the effect of preconditioning the donor liver to change HO-1 expression in IRI after LT from a cardiac-death donor. In conclusion, HO-1 can inhibit hepatocyte pyroptosis, thereby alleviating IRI after LT in SD rats. The study is limited by the fact that it only observed pyroptosis caused by HO-1; however, the specific mechanism remains unclear and requires further study.

5. Conclusions

The study selected a cardiac death rat donor model to simulate the acquisition and preservation of a clinically transplanted liver, and the study was conducted by interfering with the expression of HO-1 in the donor liver. The results showed that HO-1 could promote ischemia reperfusion recovery in SD rats after DCD liver transplantation; HO-1 overexpression inhibited hepatocyte pyroptosis, thereby alleviating ischemia-reperfusion injury after liver transplantation from a cardiac death SD rat donor.

Abbreviations

AAV, adeno-associated virus; DAMPs, damage-associated molecular patterns; DCD, donors after circulatory death; GSDMD, gasdermin D; HO-1, heme oxygenase-1; IR, ischemia-reperfusion; IRI, ischemia-reperfusion injury; LT, liver transplantation; AST, aspartate aminotransferase; PRRs, pattern recognition receptors; SD, Sprague Dawley.

Availability of Data and Materials

The datasets used and/or analysed during the current study are available from the corresponding author on reasonable request.

Author Contributions

YM, ZZ and HH designed the research study. TW and YF designed and conducted all experiments, provided all images, drafted the work and reviewed it critically for important intellectual content. XZ, YY, LJ, ZL Contributed acquisition, analysis, and interpretation of data for the work. All authors have read and agreed to the published version of the manuscript. All authors have participated sufficiently in the work and agreed to be accountable for all aspects of the work.

Ethics Approval and Consent to Participate

This study was approved by the Institutional Animal Care and Use Committee of the First Affiliated Hospital of Kunming Medical University (KMMU2020189).

Acknowledgment

Not applicable.

Funding

The study was financially supported by a grant from National Natural Science Foundation of China (No. 81960123 and 81760124). The funding body had no role in study design, data collection, analysis, and interpretation of data, and writing the manuscript.

Conflict of Interest

The authors declare no conflict of interest.

Supplementary Material

Supplementary material associated with this article can be found, in the online version, at <https://doi.org/10.31083/j.fbl2810275>.

References

- [1] Cherqui D, Ciria R, Kwon CHD, Kim KH, Broering D, Wakabayashi G, *et al.* Expert Consensus Guidelines on Minimally Invasive Donor Hepatectomy for Living Donor Liver Transplantation From Innovation to Implementation: A Joint Initiative From the International Laparoscopic Liver Society (ILLS) and the Asian-Pacific Hepato-Pancreato-Biliary Association (APHPBA). *Annals of Surgery.* 2021; 273: 96–108.
- [2] Muller X, Mohkam K, Mueller M, Schlegel A, Dondero F, Sepulveda A, *et al.* Hypothermic Oxygenated Perfusion Versus Normothermic Regional Perfusion in Liver Transplantation From Controlled Donation After Circulatory Death: First International Comparative Study. *Annals of Surgery.* 2020; 272: 751–758.
- [3] Hu C, Zhao L, Zhang F, Li L. Melatonin and its protective role in attenuating warm or cold hepatic ischaemia/reperfusion injury. *Cell Proliferation.* 2021; 54: e13021.
- [4] Mihm S. Danger-Associated Molecular Patterns (DAMPs): Molecular Triggers for Sterile Inflammation in the Liver. *International Journal of Molecular Sciences.* 2018; 19: 3104.
- [5] Linden J, Koch-Nolte F, Dahl G. Purine Release, Metabolism, and Signaling in the Inflammatory Response. *Annual Review of Immunology.* 2019; 37: 325–347.
- [6] Liu H, Man K. New Insights in Mechanisms and Therapeutics for Short- and Long-Term Impacts of Hepatic Ischemia Reperfusion Injury Post Liver Transplantation. *International Journal of Molecular Sciences.* 2021; 22: 8210.
- [7] Gaul S, Leszczynska A, Alegre F, Kaufmann B, Johnson CD, Adams LA, *et al.* Hepatocyte pyroptosis and release of inflammasome particles induce stellate cell activation and liver fibrosis. *Journal of Hepatology.* 2021; 74: 156–167.
- [8] Wang K, Sun Q, Zhong X, Zeng M, Zeng H, Shi X, *et al.* Structural Mechanism for GSDMD Targeting by Autoprocessed Caspases in Pyroptosis. *Cell.* 2020; 180: 941–955.e20.
- [9] Shi J, Zhao Y, Wang K, Shi X, Wang Y, Huang H, *et al.* Cleavage of GSDMD by inflammatory caspases determines pyroptotic cell death. *Nature.* 2015; 526: 660–665.
- [10] Zeng Z, Huang HF, Chen MQ, Song F, Zhang YJ. Contributions of heme oxygenase-1 in postconditioning-protected ischemia-reperfusion injury in rat liver transplantation. *Transplantation Proceedings.* 2011; 43: 2517–2523.
- [11] Zhou R, Yazdi AS, Menu P, Tschopp J. A role for mitochondria in NLRP3 inflammasome activation. *Nature.* 2011; 469: 221–225.
- [12] Puentes-Pardo JD, Moreno-SanJuan S, Carazo Á, León J. Heme Oxygenase-1 in Gastrointestinal Tract Health and Disease. *Antioxidants.* 2020; 9: 1214.
- [13] Ryter SW. Therapeutic Potential of Heme Oxygenase-1 and Carbon Monoxide in Acute Organ Injury, Critical Illness, and Inflammatory Disorders. *Antioxidants.* 2020; 9: 1153.
- [14] Huang HF, Zeng Z, Wang KH, Zhang HY, Wang S, Zhou WX, *et al.* Heme oxygenase-1 protects rat liver against warm ischemia/reperfusion injury via TLR2/TLR4-triggered signaling pathways. *World Journal of Gastroenterology.* 2015; 21: 2937–2948.
- [15] Qu S, Yuan B, Zhang H, Huang H, Zeng Z, Yang S, *et al.* Heme Oxygenase 1 Attenuates Hypoxia-Reoxygenation Injury in Mice Liver Sinusoidal Endothelial Cells. *Transplantation.* 2018; 102: 426–432.
- [16] Kamada N, Davies HS, Wight D, Culank L, Roser B. Liver transplantation in the rat. Biochemical and histological evidence of complete tolerance induction in non-rejector strains. *Transplantation.* 1983; 35: 304–311.
- [17] Percie du Sert N, Hurst V, Ahluwalia A, Alam S, Avey MT, Baker M, *et al.* The ARRIVE guidelines 2.0: Updated guidelines for reporting animal research. *PLoS Biology.* 2020; 18: e3000410.
- [18] Suzuki S, Toledo-Pereyra LH. Monoclonal antibody to intercellular adhesion molecule 1 as an effective protection for liver ischemia and reperfusion injury. *Transplantation Proceedings.* 1993; 25: 3325–3327.
- [19] Suzuki S, Toledo-Pereyra LH, Rodriguez FJ, Cejalvo D. Neutrophil infiltration as an important factor in liver ischemia and reperfusion injury. Modulating effects of FK506 and cyclosporine. *Transplantation.* 1993; 55: 1265–1272.
- [20] Yuan B, Huang H, Qu S, Zhang H, Lin J, Jin L, *et al.* Gastrodin Pretreatment Protects Liver Against Ischemia-Reperfusion Injury via Activation of the Nrf2/HO-1 Pathway. *The American Journal of Chinese Medicine.* 2020; 48: 1159–1178.
- [21] Fang Y, Yang Y, Zhang X, Li N, Yuan B, Jin L, *et al.* A Co-Expression Network Reveals the Potential Regulatory Mechanism of lncRNAs in Relapsed Hepatocellular Carcinoma. *Frontiers in Oncology.* 2021; 11: 745166.

- [22] Northup PG, Garcia-Pagan JC, Garcia-Tsao G, Intagliata NM, Superina RA, Roberts LN, *et al.* Vascular Liver Disorders, Portal Vein Thrombosis, and Procedural Bleeding in Patients With Liver Disease: 2020 Practice Guidance by the American Association for the Study of Liver Diseases. *Hepatology*. 2021; 73: 366–413.
- [23] Singal AK, Kwo P, Kwong A, Liangpunsakul S, Louvet A, Mandrekar P, *et al.* Research methodologies to address clinical unmet needs and challenges in alcohol-associated liver disease. *Hepatology*. 2022; 75: 1026–1037.
- [24] Hirao H, Dery KJ, Kageyama S, Nakamura K, Kupiec-Weglinski JW. Heme Oxygenase-1 in liver transplant ischemia-reperfusion injury: From bench-to bedside. *Free Radical Biology & Medicine*. 2020; 157: 75–82.
- [25] Burdette BE, Esparza AN, Zhu H, Wang S. Gasdermin D in pyroptosis. *Acta Pharmaceutica Sinica B*. 2021; 11: 2768–2782.
- [26] Zhang Q, Piao C, Ma H, Xu J, Wang Y, Liu T, *et al.* Exosomes from adipose-derived mesenchymal stem cells alleviate liver ischemia reperfusion injury subsequent to hepatectomy in rats by regulating mitochondrial dynamics and biogenesis. *Journal of Cellular and Molecular Medicine*. 2021; 25: 10152–10163.
- [27] Marra F, Tacke F. Roles for chemokines in liver disease. *Gastroenterology*. 2014; 147: 577–594.e1.